Supporting Information

A series of dinuclear Dy(III) complexes bridged by 2-methyl-8-hydroxylquinoline: replacement on periphery coordinated β-diketonate terminal leads to different single-molecule magnetic properties

Wan-Ying Zhang,[a] Yong-Mei Tian,[a] Hong-Feng Li,[a] Peng Chen,[a] Wen-Bin Sun[a,]*, Yi-Quan Zhang,[b,]* and Peng-Fei Yan[a,]*

[a.] Key Laboratory of Functional Inorganic Material Chemistry Ministry of Education, Heilongjiang University, Harbin 150080, P. R. China. E-mail: wenbinsun@126.com and yanpf@vip.sina.com

[b.] Jiangsu Key Laboratory for NSLSCS, School of Physical Science and Technology, Nanjing Normal University, Nanjing 210023, P. R. China. E-mail: zhangyiquan@njnu.edu.cn

Table S1. Selected Bond Distances (Å) and Angles (^{o}) for **1**-**4**.

1		**2**		**3**		**4**	
Dy1-O1	2.434(3)	Dy1-O1	2.3404(12)	Dy1-O1	2.3322(13)	O1-Dy1	2.342(3)
Dy1-O2	2.397(2)	Dy1-O2	2.2808(12)	Dy1-O2	2.3070(14)	O2-Dy1	2.330(3)
Dy1-O2’	2.316(2)	Dy1-O3	2.2719(14)	Dy1-O3	2.2556(15)	O3-Dy1	2.347(3)
Dy1-O3’	2.305(2)	Dy1-O4	2.2832(15)	Dy1-O4	2.2643(15)	O4- Dy1	2.360(3)
Dy1-O4’	2.330(3)	Dy1-O5	2.2602(13)	Dy1-O5	2.2849(15)	O5- Dy1	2.393(4)
Dy1-O5’	2.351(3)	Dy1-O1’	2.3001(13)	Dy1-O6	2.2579(15)	O6-Dy1	2.397(3)
Dy1-O6’	2.347(2)	Dy1-N1’	2.4943(17)	Dy1-N2	2.5621(16)	O7-Dy1	2.342(4)
Dy1-N1	2.610(3)	N1-Dy1’	2.4943(17)	Dy2-O1	2.2955(14)	Dy1-O1’	2.371(3)
O2-Dy1’	2.316(2)	Dy1-Dy1’	3.7652(3)	Dy2-O2	2.3343(13)	O1-Dy1’	2.371(3)
Dy1-Dy1’	3.9232(4)	O5-Dy1-O3	143.35(6)	Dy2-O7	2.2697(15)	Dy1-Dy1’	3.8787(5)
O2’-Dy1-O6’	88.53(8)	O3-Dy1-O2	73.34(5)	Dy2-O8	2.2632(14)	O2-Dy1-O7	135.85(13)
O3’-Dy1-O5’	78.41(9)	O3-Dy1-O4	88.68(5)	Dy2-O9	2.2845(15)	O7-Dy1-O1	144.07(12)
O4’-Dy1-O5’	79.67(9)	O5-Dy1-O1’	105.31(4)	Dy2-O10	2.2621(15)	O7-Dy1-O3	74.79(13)
O3’-Dy1-O2	146.14(9)	O2-Dy1-O1’	106.54(5)	Dy2-N1	2.5526(17)	O2-Dy1-O4	79.19(13)
O4’-Dy1-O2	134.01(8)	O5-Dy1-O1	79.66(5)	Dy1-Dy2	3.78100(15)	O1-Dy1-O4	78.26(11)
O5’-Dy1-O2	120.33(8)	O2-Dy1-O1	148.22(5)	O3-Dy1-O4	73.13(5)	O2-Dy1-O1	79.08(12)
O2’-Dy1-O1	74.33(8)	O5-Dy1-O2	129.29(6)	O3-Dy1-O5	83.89(6)	O2-Dy1-O3	71.33(12)
O6’-Dy1-O1	147.08(9)	O5-Dy1-O4	73.10(4)	O4-Dy1-O5	81.55(6)	O1-Dy1-O3	121.08(12)
O2-Dy1-O1	76.01(9)	O2-Dy1-O4	76.26(5)	O6-Dy1-O2	101.58(5)	O7-Dy1-O4	111.56(14)
O2’-Dy1-N1	129.57(9)	O3-Dy1-O1’	91.34(5)	O5-Dy1-O2	172.17(5)	O3-Dy1-O4	139.41(12)
O6’-Dy1-N1	91.42(8)	O4-Dy1-O1’	177.08(5)	O6-Dy1-O1	81.20(5)	O2-Dy1-O1’	112.83(12)
O2-Dy1-N1	65.07(8)	O3-Dy1-O1	74.99(4)	O5-Dy1-O1	114.15(5)	O1-Dy1-O1’	69.25(12)
O2’-Dy1-O4’	79.20(9)	O4-Dy1-O1	105.66(5)	O3-Dy1-N2	71.66(5)	O4-Dy1-O1	141.62(11)
O3’-Dy1-O2	108.87(8)	O1’-Dy1-O1	71.54(5)	O4-Dy1-N2	142.51(5)	O7-Dy1-O5	69.07(14)
O3’-Dy1-O4’	73.49(9)	O3-Dy1-N1’	135.74(6)	O2-Dy1-N2	66.90(5)	O3-Dy1-O5	74.87(13)
O3’-Dy1-O6’	142.08(9)	O4-Dy1-N1’	114.26(6)	O3-Dy1-O6	138.58(5)	O1’-Dy1-O5	146.15(12)
O4’-Dy1-O6’	77.34(8)	O1-Dy1-N1’	127.56(4)	O6-Dy1-O4	133.14(5)	O7-Dy1-O6	71.51(13)
O2’-Dy1-O5’	154.45(8)	O5-Dy1-N1’	80.87(6)	O6-Dy1-O5	72.37(5)	O3-Dy1-O6	141.17(12)

O6’-Dy1-O5’	72.93(9)	O2-Dy1-N1’	76.18(4)	O3-Dy1-O2	98.14(5)	O7-Dy1-O1’	85.61(12)
O2’-Dy1-O2	67.29(8)	O1’-Dy1-N1’	67.59(5)	O4-Dy1-O2	106.28(5)	O3-Dy1-O1’	77.08(11)
O6’-Dy1-O2	71.43(8)	Dy1’-O1-Dy1	108.46(5)	O3-Dy1-O1	140.13(5)	O2-Dy1-O5	75.32(14)
O3’-Dy1-O1	70.81(10)			O4-Dy1-O1	74.86(5)	O1-Dy1-O5	142.97(12)
O4’-Dy1-O1	124.78(9)			O2-Dy1-O1	68.93(4)	O4-Dy1-O5	71.04(12)
O5’-Dy1-O1	130.25(8)			O6-Dy1-N2	83.21(5)	O2-Dy1-O6	147.47(13)
O3’-Dy1-N1	101.49(9)			O5-Dy1-N2	106.90(6)	O1-Dy1-O6	79.53(12)
O4’-Dy1-N1	149.33(10)			O1-Dy1-N2	128.64(5)	O4-Dy1-O6	72.65(12)
O5’-Dy1-N1	69.73(9)			O10-Dy2-O7	140.54(6)	O1’-Dy1-O6	81.64(11)
O1-Dy1-N1	79.13(9)			O10-Dy2-O9	72.57(5)	O5-Dy1-O6	109.47(14)
Dy1’-O2-Dy1	112.71(8)			O7-Dy2-O9	84.76(6)	Dy1’-O1-Dy1	110.75(11)
				O8-Dy2-O1	101.05(5)		
				O9-Dy2-O1	170.15(5)		
				O8-Dy2-O2	142.90(5)		
				O9-Dy2-O2	109.27(5)		
				O10-Dy2-O8	134.67(5)		
				O8-Dy2-O7	72.93(5)		
				O8-Dy2-O9	86.00(6)		
				O10-Dy2-O1	97.59(5)		
				O7-Dy2-O1	103.81(6)		
				O10-Dy2-O2	82.41(5)		
				O7-Dy2-O2	75.04(5)		
				O1-Dy2-O2	69.08(4)		
				O10-Dy2-N1	79.85(6)		
				O7-Dy2-N1	139.17(5)		
				O1-Dy2-N1	66.67(5)		
				O8-Dy2-N1	70.55(5)		
				O9-Dy2-N1	109.99(6)		
				O2-Dy2-N1	129.16(5)		

Dy1-O2-Dy2	109.10(5)
Dy2-O1-Dy1	109.57(5)

Table S2. Dy(III) Geometry Analysis by SHAPE Software

Dy(III)	ideal geometries	S_{Dy}
Complex **1**	Hexagonal bipyramid (D_{6h})	24.088
	Johnson gyrobifastigium J26 (D_{2d})	24.917
	Triakis tetrahedron (T_d)	26.928
Complex **2**	Capped trigonal prism (C_{2v})	2.798
	Capped octahedron (C_{3v})	2.799
	Pentagonal bipyramid (D_{5h})	5.791
Complex **3**	Capped trigonal prism (C_{2v})	3.924
	Capped octahedron (C_{3v})	4.280
	Pentagonal bipyramid (D_{5h})	5.865
Complex **4**	Square antiprism (D_{4d})	0.449
	Triangular dodecahedron (D_{2d})	2.295
	Biaugmented trigonal prism (C_{2v})	2.321

Table S3. Best fitted parameters (χ_T, χ_S, τ and α) with the extended Debye model for complex **3** at 0 Oe in the temperature range 2-6.5 K.

T/ K	χ_S / cm^3 mol^{-1}	χ_T / cm^3 mol^{-1}	τ/s	α
2	0.12530	6.08885	0.00089	0.16669
2.25	0.15422	6.04374	0.00085	0.15565
2.5	0.24922	5.92394	0.00082	0.13345
2.75	0.24960	5.79623	0.00078	0.12918
3	0.24970	5.61771	0.00074	0.12045
3.5	0.23002	5.25504	0.00064	0.10381
4	0.25000	4.91258	0.00054	0.08129
4.5	0.20275	4.58551	0.00043	0.06791
5	0.30210	4.28910	0.00035	0.04125
5.5	0.34318	4.02184	0.00028	0.02235
6	0.34637	3.80014	0.00022	0.01937

6.5	0.39957	3.56059	0.00018	0.00003

Table S4. Best fitted parameters (χ_T, χ_S, τ and α) with the extended Debye model for complex **4** at 0 Oe in the temperature range 2-4 K.

T/ K	χ_S / cm^3 mol^{-1}	χ_T / cm^3 mol^{-1}	τ/s	α
2	1.65796	6.10008	0.00037	0.24613
2.25	1.69563	5.85936	0.00037	0.20449
2.5	1.70201	5.62123	0.00036	0.17428
2.75	1.66697	5.38899	0.00034	0.15277
3	1.64410	5.17192	0.00032	0.13030
3.5	1.64181	4.74499	0.00026	0.08930
4	1.68097	4.36980	0.00019	0.06766

Table S5. Best fitted parameters (χ_T, χ_S, τ and α) with the extended Debye model for complex **1** at 2000 Oe in the temperature range 2-8 K.

T/ K	χ_S / cm^3 mol^{-1}	χ_T / cm^3 mol^{-1}	τ/s	α
2.5	0.11997	7.31930	0.03808	0.30000
3	0.12000	6.95000	0.03193	0.29990
3.5	0.11972	6.32544	0.02332	0.29928
4	0.11945	5.60220	0.01454	0.25573
4.5	0.11998	5.02314	0.00881	0.21556
5	0.11984	4.58851	0.00543	0.18532
5.5	0.11996	4.23031	0.00329	0.16375
6	0.11920	3.90386	0.00195	0.14860
6.5	0.11986	3.65929	0.00113	0.14970
7	0.10663	3.43639	0.00063	0.15557
7.5	0.35534	3.21339	0.00037	0.10809
8	0.53411	3.02829	0.00021	0.09632

Table S6. Best fitted parameters (χ_T, χ_S, τ and α) with the extended Debye model for complex **2** at 1900 Oe in the temperature range 2-4.5 K.

T/ K	χ_S / cm^3 mol^{-1}	χ_T / cm^3 mol^{-1}	τ/s	α
2	0.60000	10.12839	0.00493	0.29944
2.5	0.63680	9.06795	0.00222	0.25706

3	0.69680	8.40000	0.00104	0.23214
3.5	0.99315	7.45765	0.00050	0.15612
4	1.09983	6.90019	0.00028	0.16029
4.5	1.74336	6.40244	0.00019	0.14520

Table S7. Best fitted parameters (χ_T, χ_S, τ and α) with the extended Debye model for complex **3** at 1900 Oe in the temperature range 2-7.5 K.

T/ K	χ_S / cm^3 mol^{-1}	χ_T / cm^3 mol^{-1}	τ/s	α
2	0.19901	7.07782	0.10006	0.25626
2.5	0.26395	6.90062	0.05013	0.23232
3	0.30000	5.87184	0.01647	0.15659
3.5	0.12916	5.35453	0.00644	0.16267
4	0.07079	4.91269	0.00295	0.13722
4.5	0.11987	4.60001	0.00164	0.09900
5	0.14100	4.22909	0.00097	0.05548
5.5	0.08867	3.94704	0.00062	0.03895
6	0.19523	3.72780	0.00044	0.01148
6.5	0.18833	3.51565	0.00032	0.00511
7	0.26244	3.33593	0.00024	0.00012
7.5	0.30160	3.16749	0.00019	0.00345

Table S8. Best fitted parameters (χ_T, χ_S, τ and α) with the extended Debye model for complex **4** at 1500 Oe in the temperature range 2-4 K.

T/ K	χ_S / cm^3 mol^{-1}	χ_T / cm^3 mol^{-1}	τ/s	α
2	1.23529	6.60260	0.00438	0.30000
2.25	1.09989	6.37297	0.00339	0.30000
2.5	1.05631	6.15053	0.00267	0.30000
2.75	0.93170	5.89968	0.00194	0.29997
3	0.96708	5.60012	0.00141	0.25638
3.25	1.20000	5.30580	0.00106	0.18222
3.5	1.10181	5.10062	0.00073	0.17398
3.75	1.11077	4.86307	0.00050	0.14640

4	1.19125	4.66218	0.00035	0.12299
4.25	1.2038	4.48013	0.00023	0.12579

Table S9 The curves are fitted by the modified Arrhenius relationship the QTM process is taken account $1/\tau = 1/\tau_{QTM}+\tau_0^{-1}\exp(-U_{eff}/k_BT)$

complex	q (s)	U_{eff}/k_B (K)	τ_0 (s)
3	8.7×10^{-4}	20.0	1.0×10^{-5}
4	3.5×10^{-4}	20.4	2.0×10^{-6}

Table S10 The curves are fitted by the modified Arrhenius relationship the Raman process is taken account $1/\tau = CT^n + \tau_0^{-1}\exp(-U_{eff}/k_BT)$

complex	C ($s^{-1}\cdot K^{-n}$)	n	τ_0 (s)	U_{eff}/k_B (K)
1	0.76	3.4	2.1×10^{-8}	75.6
2	47.3	1.4	2.9×10^{-6}	18.6
3	2.6	2.1	6.1×10^{-6}	25.8
4	53.2	1.7	4.7×10^{-7}	26.9

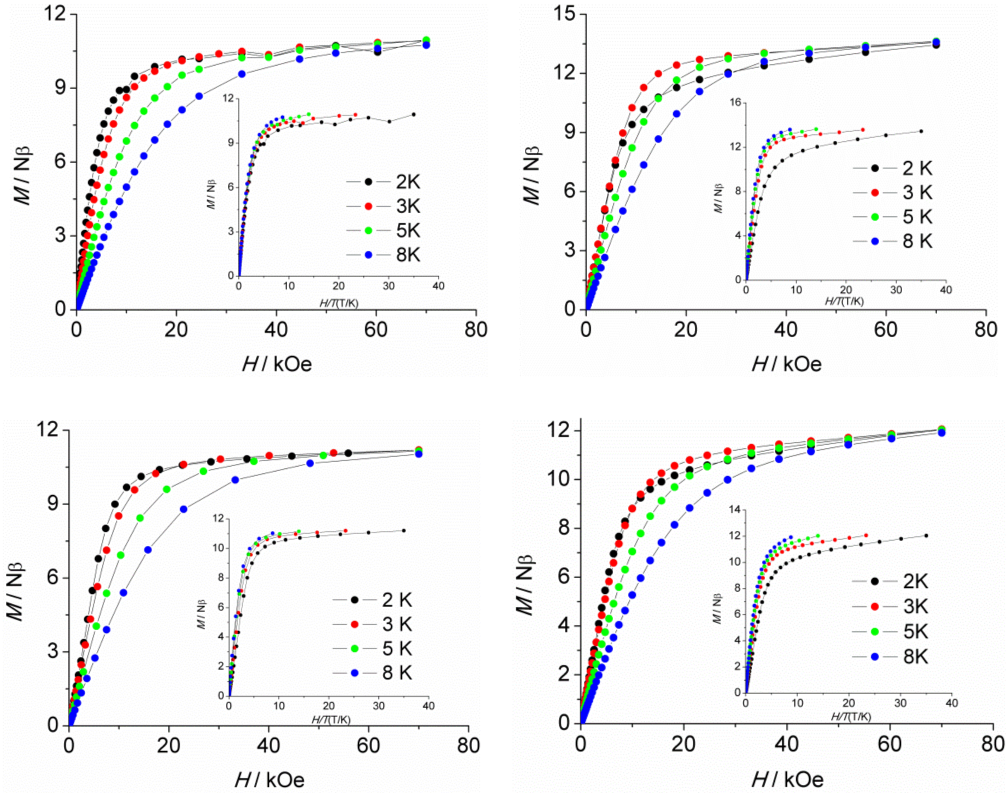

Fig. S1 Molar magnetization versus field at 2-8 K. Inset: Experimental M vs. H/T plots at 2-8 K for complexes **1** (top, left), **2** (top, right), **3** (down, left) and **4** (down, right).

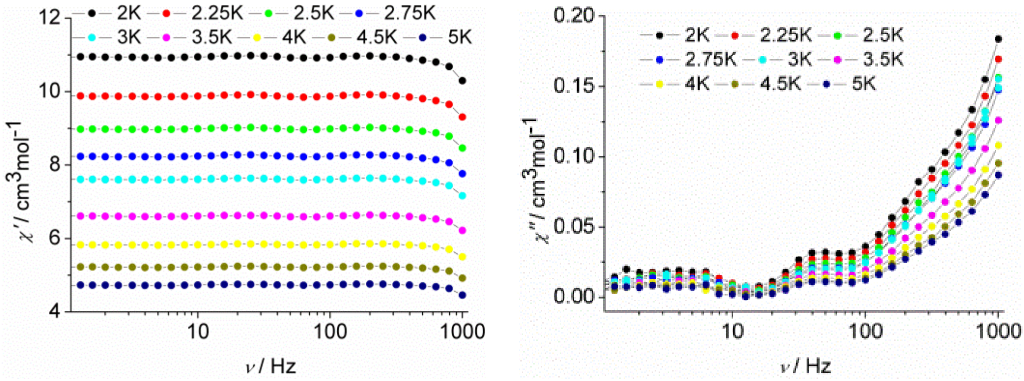

Fig. S2 Frequency dependence of the in-phase (χ′) ac susceptibility (left) and the out-of-phase (χ′′) ac susceptibility (right) in temperature range 2-5 K of complex **1** under 0 Oe.

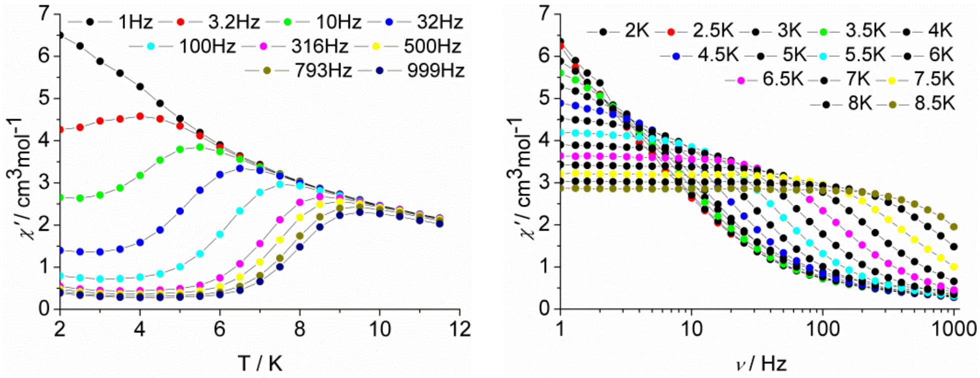

Fig. S3 Temperature dependence of the in-phase (χ′) ac susceptibility in the frequency range 1-1000 Hz (left) and frequency dependence of the in-phase (χ′) ac susceptibility in the temperature range 2-8.5 K (right) of complex **2** under 0 Oe.

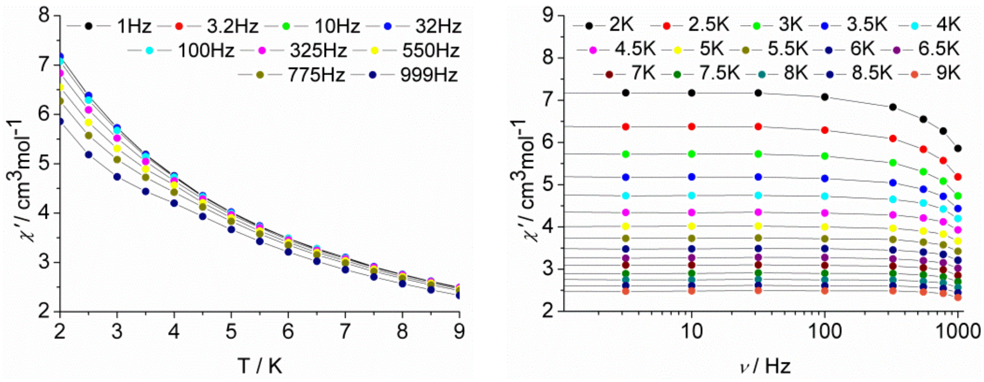

Fig. S4 Temperature dependence of the in-phase (χ′) ac susceptibility in the frequency range 1-1000 Hz (left) and frequency dependence of the in-phase (χ′) ac susceptibility in the temperature range 2-9 K (right) of complex **3** under 0 Oe.

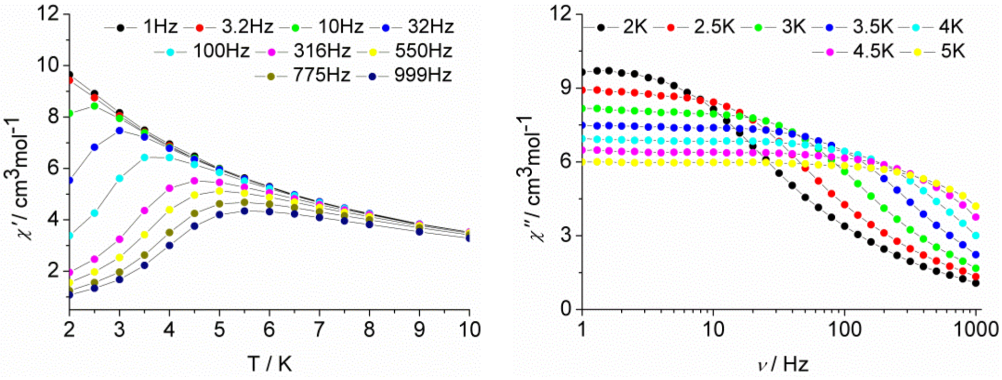

Fig. S5 Temperature dependence of the in-phase (χ') ac susceptibility in the frequency range 1-1000 Hz (left) and frequency dependence of the in-phase (χ') ac susceptibility in the temperature range 2-5 K (right) of complex **4** under 0 Oe.

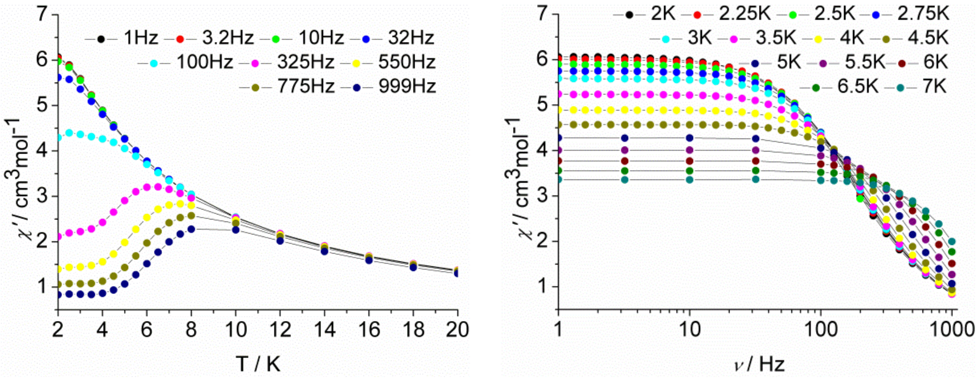

Fig. S6 Temperature dependence of the in-phase (χ') ac susceptibility in the frequency range 1-1000 Hz (left) and frequency dependence of the in-phase (χ') ac susceptibility in the temperature range 2-7 K (right) of complex **1** under 2000 Oe.

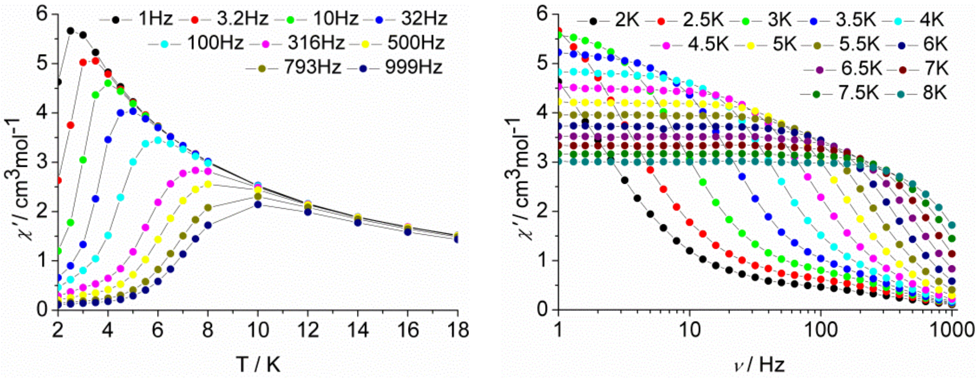

Fig. S7 Temperature dependence of the in-phase (χ') ac susceptibility in the frequency range 1-1000 Hz (left) and frequency dependence of the in-phase (χ') ac susceptibility in the temperature range 2-7 K (right) of complex **2** under 1900 Oe.

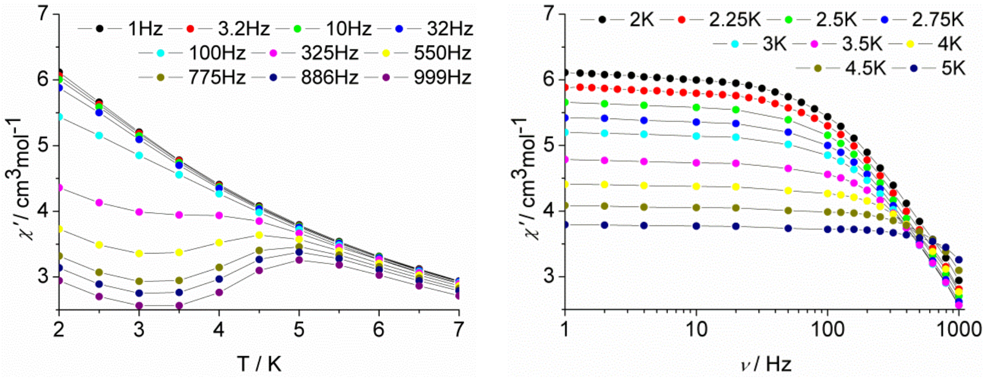

Fig. S8 Temperature dependence of the in-phase (χ′) ac susceptibility in the frequency range 1-1000 Hz (left) and frequency dependence of the in-phase (χ′) ac susceptibility in the temperature range 2-5 K (right) of complex **3** under 1900 Oe.

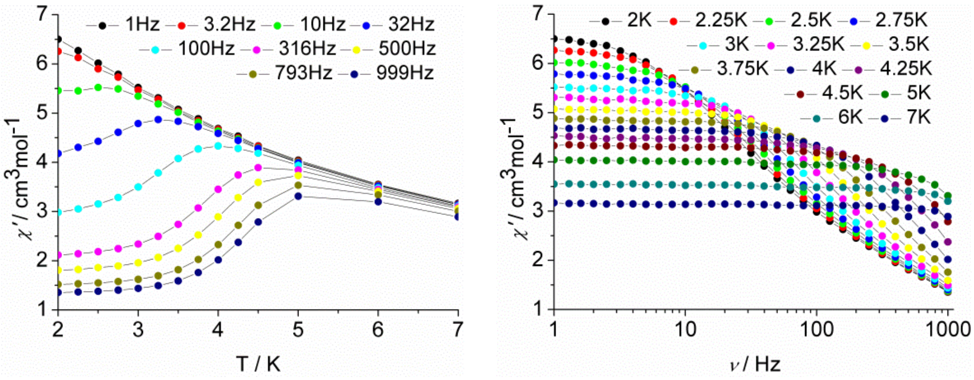

Fig. S9 Temperature dependence of the in-phase (χ′) ac susceptibility in the frequency range 1-1000 Hz (left) and frequency dependence of the in-phase (χ′) ac susceptibility in the temperature range 2-7 K (right) of complex **4** under 1300 Oe.

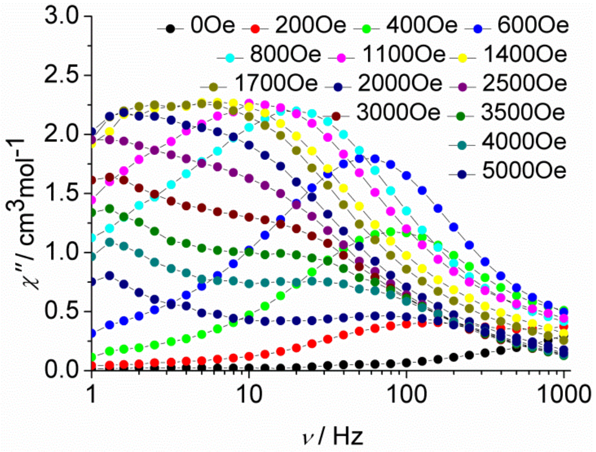

Fig. S10 Plot of the frequency dependence of the out-of-phase (χ'') ac susceptibility component under indicated dc field for complex **1.**

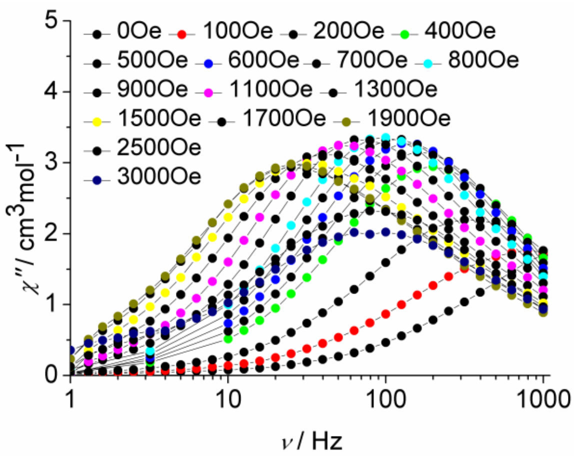

Fig. S11 Plot of the frequency dependence of the out-of-phase (χ'') ac susceptibility component under indicated dc field for complex **2.**

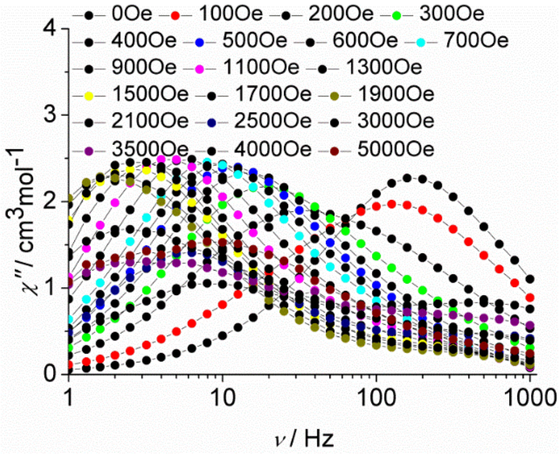

Fig. S12 Plot of the frequency dependence of the out-of-phase (χ'') ac susceptibility component under indicated dc field for complex **3.**

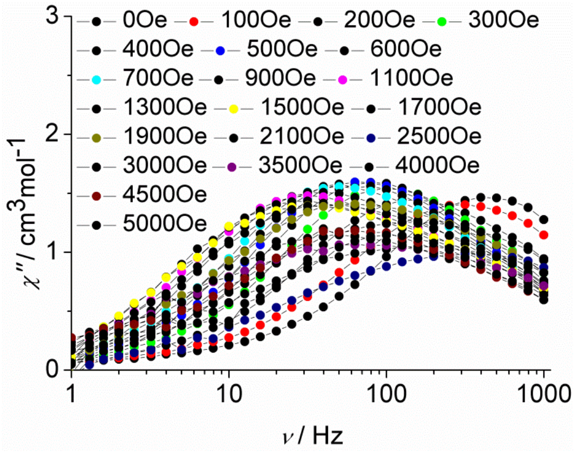

Fig. S13 Plot of the frequency dependence of the out-of-phase (χ'') ac susceptibility component under indicated dc field for complex **4.**

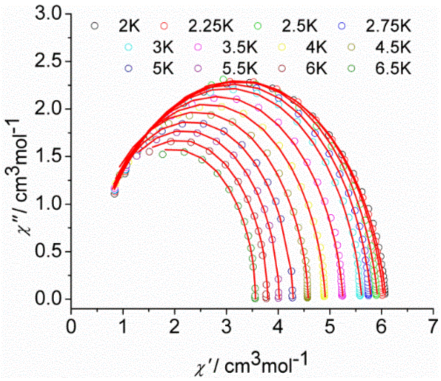

Fig. S14 Cole-Cole (Argand) plot for complex **3** obtained using the ac susceptibility data under zero dc field. The solid lines correspond to the best fit obtained with a generalized Debye model.

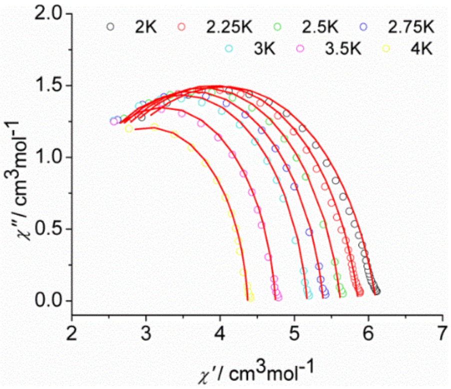

Fig. S15 Cole-Cole (Argand) plot for complex **4** obtained using the ac susceptibility data under zero dc field. The solid lines correspond to the best fit obtained with a generalized Debye model.

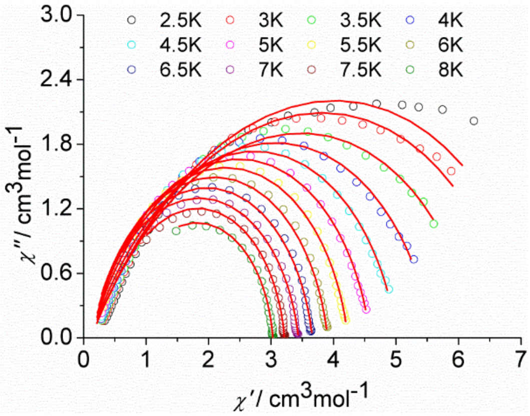

Fig. S16 Cole-Cole (Argand) plot for complex **1** obtained using the ac susceptibility data under 2000 Oe. The solid lines correspond to the best fit obtained with a generalized Debye model.

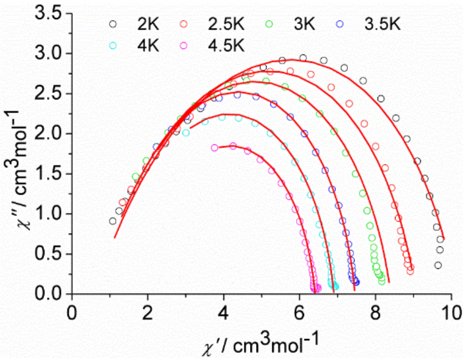

Fig. S17 Cole-Cole (Argand) plot for complex **2** obtained using the ac susceptibility data under 1900 Oe. The solid lines correspond to the best fit obtained with a generalized Debye model.

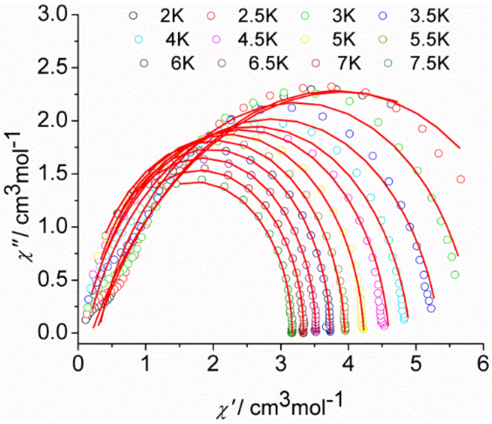

Fig. S18 Cole-Cole (Argand) plot for complex **3** obtained using the ac susceptibility data under 1900 Oe. The solid lines correspond to the best fit obtained with a generalized Debye model.

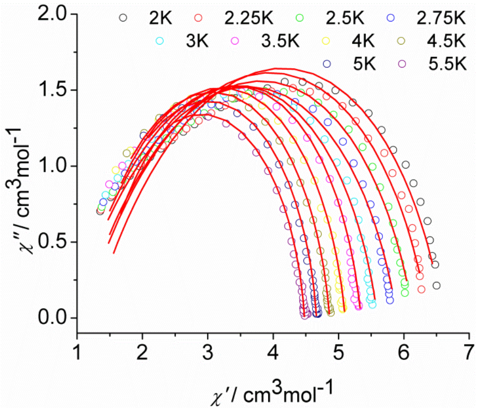

Fig. S19 Cole-Cole (Argand) plot for complex **4** obtained using the ac susceptibility data under 1500 Oe. The solid lines correspond to the best fit obtained with a generalized Debye model.

Computational details

Complete-active-space self-consistent field (CASSCF) calculations on individual lanthanide Dy^{3+} fragment of the model structures (please reference Fig. S for the models) on the basis of X-ray determined geometry have been carried out with MOLCAS 7.8 program package.[S1]

During the calculations, the other Dy^{3+} ion for each complex was replaced by diamagnetic Lu^{3+}. The basis sets for all atoms are atomic natural orbitals from the MOLCAS ANO-RCC library: ANO-RCC-VTZP for Dy^{3+} ions; VTZ for close O and N; VDZ for distant atoms. The calculations employed the second order Douglas-Kroll-Hess Hamiltonian, where scalar relativistic contractions were taken into account in the basis set and the spin-orbit couplings were handled separately in the restricted active space state interaction (RASSI-SO) procedure. For the fragment of Dy^{3+}, active electrons in 7 active spaces include all *f* electrons (CAS(9 in 7) in the CASSCF calculation. We have mixed the maximum number of spin-free state which was possible with our hardware (all from 21 sextets, 128 from 224 quadruplets, 130 from 490 doublets for the Dy^{3+} fragment).

To fit the exchange interactions in four complexes, we took two steps to obtain them. Firstly, we calculated one Dy^{3+} fragment using CASSCF to obtain the corresponding magnetic properties. And then, the exchange interaction between the magnetic centers is considered within the Lines model,[S2] while the account of the dipole-dipole magnetic coupling is treated exactly. The Lines model is effective and has been successfully used widely in the research field of f-element single-molecule magnets.[S3]

For each of complexes **1**–**4**, there is only one type of J .

The exchange Hamiltonian is:

$$\widehat{H}_{exch} = -J^{total}\,\hat{\tilde{S}}_{Dy1}\,\hat{\tilde{S}}_{Dy2} \qquad \text{(S1)}$$

The J^{total} is the parameter of the total magnetic interaction ($J^{total} = J^{diploar} + J^{exchange}$) between magnetic center ions. The $\hat{\tilde{S}}_{Dy}$ = ±1/2 are the ground pseudospin on the Dy^{3+} sites for **1**–**3**. For **4**, we consider the spin of the Dy^{3+} as 5/2. The dipolar magnetic coupling can be calculated exactly, while the exchange coupling constants were fitted through comparison of the computed and measured magnetic susceptibility and molar magnetization using the POLY_ANISO program.[S4]

Table S11 Energies (cm^{-1}) and ***g*** (g_x, g_y, g_z) tensors of the lowest spin-orbit states on one Dy^{3+} fragment of **1**–**4**.

1		**2**		**3a**		**3b**		**4**	
E	***g***	***E***	***g***	***E***	***g***	***E***	***g***	***E***	***g***
0	0.029	0	0.034	0	0.067	0	0.076	0	0.217
	0.056		0.108		0.109		0.135		2.528
	19.577		19.339		19.581		19.593		14.222
66.1	0.717	87.0	0.867	114.2	0.489	187.2	1.402	17.2	0.072
	1.430		1.150		0.657		3.411		2.627
	18.247		17.917		18.815		15.133		13.468
101.6	2.450	158.4	4.950	187.0	9.645	215.1	0.094	66.1	2.033
	3.245		5.520		6.733		5.018		4.482
	13.815		9.782		3.577		9.982		12.045
147.9	8.743	212.9	0859	226.9	2.006	290.9	0.911	86.3	9.154
	5.511		4.152		3.731		2.416		5.216
	0.314		9.699		11.423		12.798		0.312
208.1	3.233	304.0	1.766	301.5	3.604	322.2	8.023	114.7	3.11
	5.821		2.399		6.561		5.673		4.074
	9.304		11.888		10.069		0.817		11.492
279.2	1.546	386.6	0.080	351.6	1.355	386.8	3.262	151.3	0.012
	2.264		0.621		1.804		4.959		0.675
	15.115		15.036		14.719		11.782		17.206
473.7	0.194	506.4	0.256	564.4	0.393	606.4	0.939	190.2	0.338
	0.374		0.542		1.064		4.205		0.845
	17.445		18.651		17.121		14.084		18.976
529.0	0.129	604.4	0.116	613.1	0.267	646.7	0.622	392.5	0.051
	0.557		0250		1.427		4.963		0.065
	19.438		19.015		17.918		15.288		19.756

The intermolecular interactions zJ' of **1**–**4** were set to –0.02, –0.02, 0.21 and –0.15 cm^{-1}, respectively.

Table S12. Fitted exchange coupling constants J^{exch}, the calculated dipole-dipole interactions J^{dipolar} and the total J between Dy^{3+} ions in **1**–**4** (cm^{-1})

		1	**2**	**3**	**4**
J	J^{dipolar}	1.2	−2.6	−2.4	0.07
	J^{exch}	–0.75	0.50	−4.37	0.93
	J	0.45	−2.1	−6.8	1.0

Table S13. Angles (°) between two easy axis on Dy1 and Dy1′ (or Dy2) by ab initio

	Angles (°) between two easy axis	Angles (°) between easy axis on Dy1 and Dy1-Dy1′ (or Dy2)	Angles (°) between easy axis on Dy1′ (or Dy2) and Dy1-Dy1′ (or Dy2)
1	0	46.42	46.42
2	0	77.61	77.61
3	28.9	78.64	81.24
4	0	31.11	31.11

Table S14. Exchange energies (cm^{-1}) and main values of the g_z for the lowest two exchange doublets.

	1		**2**		**3**		**4**	
	Energy	g_z	Energy	g_z	Energy	g_z	Energy	g_z
1	0	39.154	0	0	0	9.781	0.047	29.934
2	0.236	0	1.079	38.678	3.526	37.929	6.645	0

Table S15. Angles (°) between two easy axis on Dy1 and Dy1′ (or Dy2) calculated by MAGELLAN

	Angles (°) between two easy axis	Angles (°) between easy axis on Dy1 and Dy1-Dy1′ (or Dy2)	Angles (°) between easy axis on Dy1′ (or Dy2) and Dy1-Dy1′ (or Dy2)
1	0	28.25	28.22
2	0	76.46	76.55
3	31.62	85.10	82.96
4	0	81.68	81.68

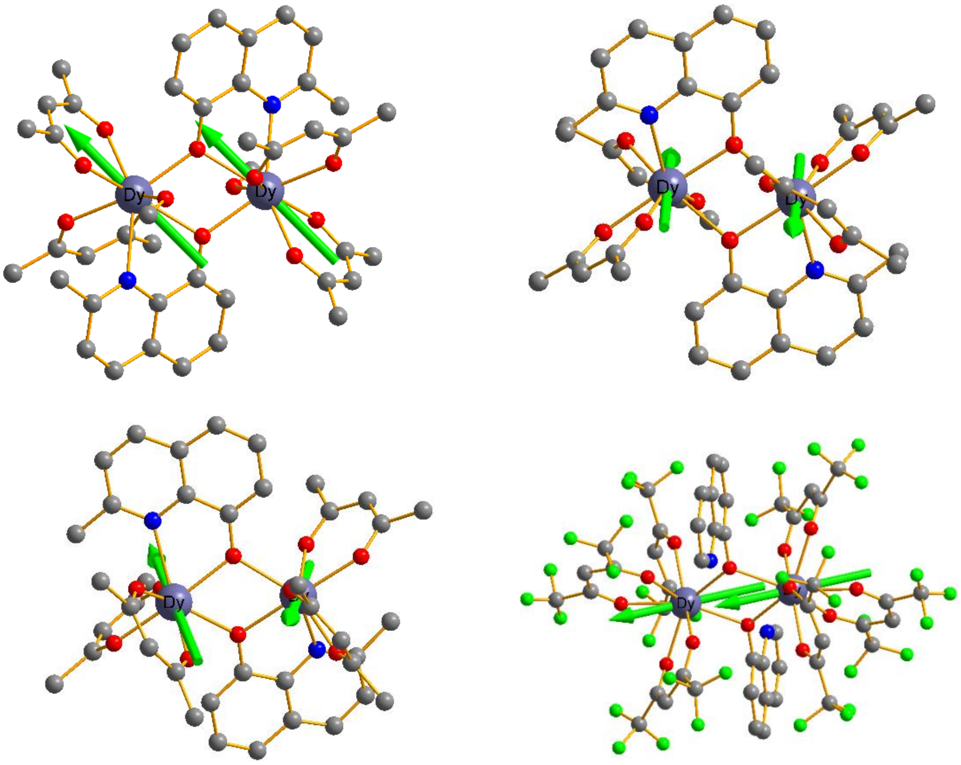

Fig. S20. Orientations of the local main magnetic axes of the ground doublets on Dy(III) ions of **1** (top, left), **2** (top, right), **3** (bottom, left) and **4** (bottom, right) as calculated by ab initio calculation.

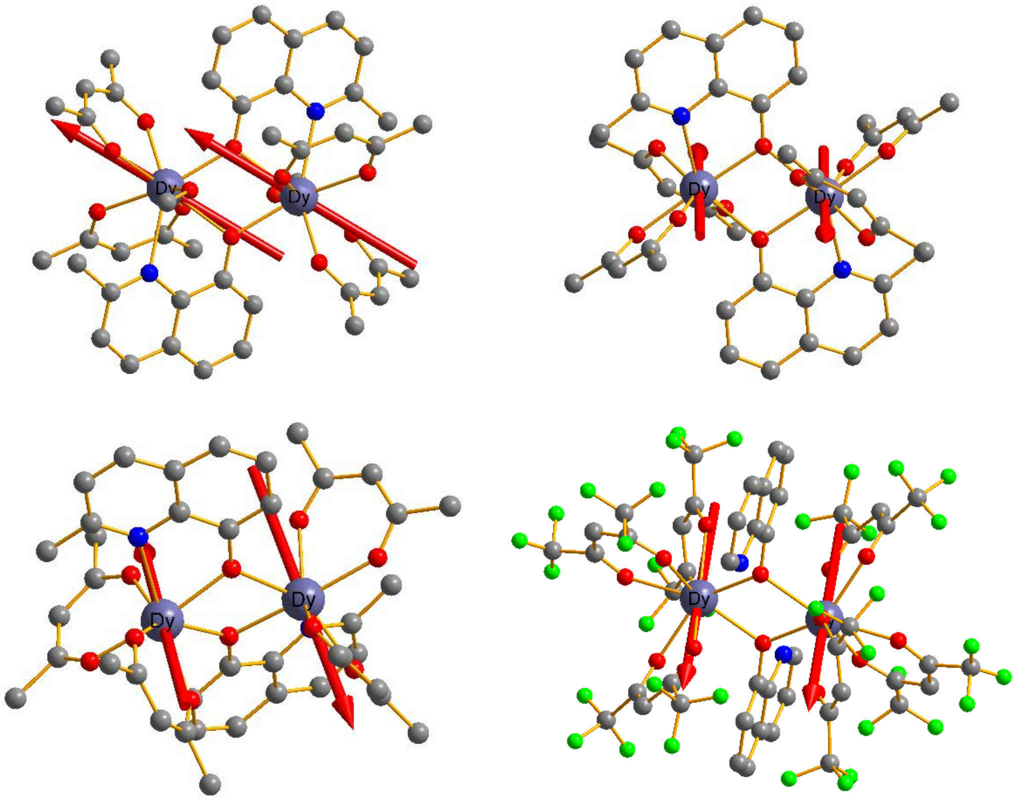

Fig. S21. Orientations of the anisotropy axes for each of the two Dy(III) ions in complexes **1** (top, left), **2** (top, right), **3** (bottom, left) and **4** (bottom, right) as calculated by MAGELLAN.

References:

S1 G. Karlström, R. Lindh, P.-Å. Malmqvist, B. O. Roos, U. Ryde, V. Veryazov, P.-O. Widmark, M. Cossi, B. Schimmelpfennig, P. Neogrady and L. Seijo, MOLCAS: a Program Package for Computational Chemistry, *Comput. Mater. Sci.*, 2003, **28**, 222.

S2 M. E. Lines, *J. Chem. Phys.*, 1971, **55**, 2977.

S3 (a) K. C. Mondal, A. Sundt, Y. H. Lan, G. E. Kostakis, O. Waldmann, L. Ungur, L. F. Chibotaru, C. E. Anson and A. K. Powell, *Angew. Chem. Int. Ed.*, 2012, ***51***, 7550; (b) S. K. Langley, D. P. Wielechowski, V. Vieru, N. F. Chilton, B. Moubaraki, B. F. Abrahams, L. F. Chibotaru and K. S. Murray, *Angew. Chem. Int. Ed.,* 2013, **52**, 12014.

S4 (a) L. F. Chibotaru, L. Ungur and A. Soncini, *Angew. Chem. Int. Ed.*, 2008, **47**, 4126; (b) L. Ungur, W. Van denHeuvel and L.F. Chibotaru, *New J. Chem.*, 2009, **33**, 1224; (c) L. F. Chibotaru, L. Ungur, C. Aronica, H. Elmoll, G. Pilet and D. Luneau, *J. Am. Chem. Soc.*, 2008, **130**, 12445.